

Host (nano cage NaY)/guest Mn(II), Co(II), Ni(II) and Cu(II) Complexes of N,N-bis(3,5-di-tert-butylsalicydene)-2,2-dimethyle-1,3-diaminopropane: Synthesis and Catalyst Activity

M. Zendehtdel,* H. Khanmohamadi and M. Mokhtari

Department of Chemistry, College of Science, Arak University, Arak, Iran

Mn(II), Co(II), Ni(II) and Cu(II) and N,N-bis(3,5-di-tert-butylsalicydene)-2,2-dimethyle-1,3-diaminopropane complexes have been synthesized in Y zeolite cavity by the reaction of ion-exchanged metal ions with the flexible ligand molecules. The host-guest materials obtained have been characterized by elemental analysis, XRD, surface area, pore volume, TGA, FT-IR and UV-Vis techniques. Analysis of data indicates that formation of complexes in the pores Y zeolite without affecting the zeolite framework structure. Also, we report the oxidation of cyclohexanol catalyzed by host-guest catalyst with tert-butyl hydrogen peroxide as oxygen donor. The activity of benzyl alcohol oxidation decreases in the series- $[Co(L)]/NaY > [Cu(L)]/NaY > [Mn(L)]/NaY > [Ni(L)]/NaY$ and the percent of product completely depend to catalyst. Zeolite complexes are stable enough to be reused and are suitable to be utilized as partial oxidation catalysts.

Keywords: Zeolite; Schiff base; Flexible ligand method; Benzyl alcohol; Oxidation.

INTRODUCTION

The zeolites are a crystalline aluminosilicates with well defined channel and cavity that these cavities contain metal cations and removable water. One of the good pores structure is Y zeolite consist almost spherical 12 Å cavities.¹ Recently one of the most subject of the heterogeneous catalyst research are nanocomposite materials that inclusive Host (nano pores zeolite or others molecular sieves) and Guest (transition metal complexes). There are many of complexes and metal Schiff-base complexes incorporated onto zeolite that such of complexes are synthesized in the super cage of zeolite just like building a ship in bottle. There have been three main approaches to preparation of these ship in bottle chelate complexes, namely I) a flexible ligand method (synthesized of metal complex in situ in the zeolite cavity by reaction of the ligand with the exchanged metal cations) that the ligand must be able to diffuse freely through the zeolite pores. The shaped complex becomes too large and rigid to escape from the cage.²⁻⁵ II) The template synthesis method (condensation of ligand inside a zeolite modified with the metal ion to be complexes). The template synthesis method is exemplified by preparation of intra zeolite mettalocyanines in this case because of the

ligand size.⁶⁻⁹ III) a zeolite synthesised methods (synthesis of the zeolite in the presence of the performed metal complex). The newest zeolite synthesis method has the obvious advantage that the nature of the intra zeolite species is well defined and no free ligand need to be removed.¹⁰

Recently, we can see in the many work that encapsulated of transition metal complexes (especially Schiff-base complexes) using in many of work. For example, this complex/zeolite has been used for degradation of dye pollution from waste water with using oxidation reaction.¹¹ In other works, these incorporated metal complexes onto zeolite can be used for preparation electrode in many of characterization.¹² Also in the several of recent work, many authors synthesised complexes of transition metal with polydentate ligand, and have characterized structure and investigated about redox properties of these materials in the solution.¹³⁻¹⁸ In this work, we report the synthesis and characterized Mn(II), Co(II), Ni(II) and Cu(II) complexes of N,N-bis(3,5-di-tert-butylsalicydene)-2,2-dimethyle-1,3-diaminopropane that incorporated onto nano dimensional pores of NaY zeolite. Hence, we report the oxidation of cyclohexanol catalyzed by host-guest nano composite with tert-butyl hydrogen peroxide as oxygen donor.

* Corresponding author. E-mail: m-Zendehtdel@araku.ac.ir; mojganzendehtdel@yahoo.com

EXPERIMENTAL

1. Material and physical measurement

All of materials and solvent were purchased from Merck. NaY zeolite¹⁹ and 3,5-di-tert-butyl-2-hydroxybenzaldehyde has been prepared according to the method reported in the literature.²⁰ All newly prepared zeolites were characterized using X-Ray diffract meter (Philips 8440) with radiation *Cu-K α* ¹⁹ at room temperature, with X-Ray diffract meter (Philips 8440), FT-IR (Galaxy series FT-IR 5000 spectrometer) TGA-DSC (Rheometric scientific STA-1500 thermo gravimetric analyzer), BET (SIBATA, App. 1100-SA with adsorption of nitrogen at 77 K), ¹H and ¹³C {¹H}NMR spectra were obtained with a Bruker Avance 300 MHz spectrometer and Diffuse reflectance spectra recorded by a UV-2100 Shimadzu Spectrophotometer.

2. Preparation of N,N-bis(3,5-di-tert-butylsalicylidene)-2,2-dimethyle-1,3-diaminopropan

A solution of 2,2-dimethyle-1,3-diaminopropan (1 mmol) in absolute EtOH (10 mL) was added to a stirring solution of 3,5-di-tert-butyl-2-hydroxybenzaldehyde (2 mmol) in absolute EtOH at 50 °C over a period of 15 min. The solution was heated in water bath over a period of 2 h at 70 °C, then cooled and let to stand at 0 °C. The obtained yellow solid was filtered off, washed with cooled n-hexane:methanol (4:1) and dried in air. The characterization data of synthesized compounds are given below. Yield 90%. m.p. = 190-192 °C. IR (KBr) $\nu_{\max}/\text{cm}^{-1}$: 1632, 1600, 1464, 1275. ¹H NMR, ppm, δ_{H} : 13.98 (br, 2H), 8.44 (s, 2H), 7.44 (d, 2H), 7.19 (br, 2H), 3.50 (s, 4H), 1.50 (s, 18H), 1.34 (s, 18H), 1.14 (s, 6H). ¹³C {¹H} NMR, ppm, $\delta_{13\text{C}}$: 166.9, 158.2, 140.1, 136.8, 127.1, 126.0, 117.9, 68.2, 36.4, 35.1, 34.2, 31.6, 29.5, 24.6. λ_{\max} (nm) (ϵ ($\text{M}^{-1}\text{cm}^{-1}$)) in CHCl₃: 270 (12650), 326 (11970), 431 (430). Anal. Calc. for C₃₅H₅₄N₂O₂: C, 78.60; H, 10.18; N, 5.24%. Found: C, 78.5; H, 10.3; N, 5.4%.

3. Preparation of M(II) NaY (M = Mn, Co, Ni and Cu)

Metal ions incorporated onto the zeolite using ion-exchange in aqueous solution as reported previously.²¹ Typically, 2 mmol of metal chloride was dissolved in 200 mL deionized water. The 2 g of NaY zeolite was added to it and stirred for 24 h at room temperature. Solid product was filtered and washed with deionized water until the product was free from metal ion on the surface of the zeolite, and dried at 100 °C.

4. Preparation of [M complex]-NaY

For preparation of [M complex]-NaY to 100 mL of

stirred methanol 4 g of M(II) NaY and 0.37 g of H₂L were added and then refluxed for 8 h. The solid consisting of M (Schiff-base) dented as M (Schiff-base)-NaY was collected by filtration washed with ethanol until unreacted ligand removed. The uncomplexed M(II) ions present in the zeolite were removed by exchanging with aqueous 0.01 M sodium nitrate solution. The resulting solid were dried, characterized and use for oxidation.

5. Oxidation of alcohol, general procedure

A mixture of catalysts (0.05 g) and 1 mL of Benzyl alcohol in acetonitril (15 mL) were stirred. Then 2 mL of TBHP (tert-buthyl, hydrogen peroxide) was added to it. The resulting mixture was then reflux for 8 hours. After filtration the solid was washed with solvent. The product subjected to GC analysing using a GC gas chromatograph Perkin-Elmer 1800 that equipped with a packed column OV-17 (1.5 m in length) and a flame ionization detector (FID).

RESULT AND DISCUSSION

X-ray Diffraction

XRD patterns indicated that the metal-exchange zeolites and zeolite complexes almost alike that of the parent NaY zeolite. Also no crystalline pattern was seen for the encapsulated complex, this might be because of their fine distribution in the lattice. It appears that the metal exchange and encapsulation condition have little effect on the crystalline of zeolite host.²²

Analytical data

Analytical data for NaY, M(II)Y and M(Schiff base)/NaY show in Table 1. Result show that percent of C, N, H, Si and Al are almost similar to alone ligand and NaY zeolite. The parent NaY zeolite has Si/Al molar ratio of 2.30 which corresponds to a unit cell formula Na₅₆[(AlO₂)₅₆(SiO₂)₁₃₆]. The analytical data for C, H, N and M(II) show that the complexes have mononuclear structure. In all of samples ratio of Si/Al has remained unchanged, indicating the absence of dealumination during ion exchange. The unit cell formulae of metal-exchanged zeolites show a metal dispersion of around 9~12 moles per unit cell, Na_{33.5}Mn_{11.2}[(AlO₂)₅₆(SiO₂)₁₃₆].*n*H₂O; Na_{31.1}Co_{12.4}[(AlO₂)₅₆(SiO₂)₁₃₆].*n*H₂O; Na_{30.8}Ni_{12.6}[(AlO₂)₅₆(SiO₂)₁₃₆].*n*H₂O; Na_{37.4}Cu_{9.7}[(AlO₂)₅₆(SiO₂)₁₃₆].*n*H₂O). The analytical data of each complex indicate M:C:H molar ratios almost close to those calculated for the mononuclear struc-

Table 1. Analytical data for NaY, M(II) Y and M (Schiff base)/NaY

Catalyst	Colour	%M	%C	%N	%H	C/N	%Si	%Al	%Na	Si/Al
NaY	White	-	-	-	-	-	20.55	8.94	7.22	2.30
Mn-NaY	Bright pink	2.96	-	-	-	-	20.78	9.03	3.62	2.30
[MnL]-NaY	Bright brown pinkish	2.88	2.24	0.11	0.20	14.96	20.60	8.95	5.12	2.30
Co-NaY	Pink	3.28	-	-	-	-	20.80	9.04	3.33	2.30
[CoL]-NaY	Orange	3.20	2.10	0.14	0.44	15.00	20.57	8.96	4.83	2.30
Ni-NaY	Bright green	3.33	-	-	-	-	20.83	9.07	3.29	2.30
Ni(L)/NaY	Pale yellow	3.24	2.25	0.15	0.30	14.98	20.37	8.80	4.74	2.30
Cu-NaY	Bright blue	2.53	-	-	-	-	20.73	9.01	3.73	2.30
Cu(L)/NaY	Green blue	2.45	2.10	0.14	0.22	15.00	20.41	8.85	5.25	2.30

ture. However, the presence of minute traces of free metal ions in the lattice could be assumed as the metal content is slightly higher than the stoichiometric requirement. Only a portion of metal ions in metal-exchanged zeolite has undergone complexation and the rest is expected to be removed on re-exchange with sodium nitrate solution. The results show that there are free metals ions in the lattice. These free metal ions which could not be re-exchanged due to the barrier by the molecules are not expected to cause any serious interference in the behaviour of encapsulated complexes.

Surface area (BET)

Table 2 shows BET of the catalysts are investigated. In comparison to the host material, a decrease in the BET surface area and the nanoporous volumes can be detected with all catalysts. The lowering surface area indicates the presence of M (Schiff-base) complex within the cavity of zeolites and not on the external zeolite.

FT-IR and DRS

Table 3 shows results for FT-IR and DRS from M

Table 2. Surface area and pore volume data of complexes encapsulated in nanoporous of zeolite Y

Sample	Surface area (m ² /g)	Pore volume (mL/g)
NaY	560	0.33
Mn(II)-NaY	546	0.31
[MnL]-NaY	417	0.23
Co(II)-NaY	542	0.31
[CoL]-NaY	412	0.21
Ni(II)-NaY	540	0.31
[NiL]-NaY	416	0.23
Cu(II)-NaY	543	0.31
[CuL]-NaY	413	0.21

(Schiff base)/zeolite. Although, the FT-IR bands for M (Schiff-base) complex due to their low concentration in the zeolite are weak. But IR spectra of all the hybrid materials showed an intense band at ca. 1009 cm⁻¹ attributable to the asymmetric stretching of Al-O-Si chain of zeolite. The symmetric stretching and bending frequency bands of Al-O-Si framework of zeolite appear at ca. 745 and 440 cm⁻¹, respectively²³ that transition metal/complexes encap-

Table 3. The DRS and FT-IR data of the free H₂L₂ ligand, NaY and M(L)/NaY

Sample	Internal vibrations			External vibration		νC=N (cm ⁻¹)	d-d (nm)
	vasym T-O	vsym T-O	T-O bend	D-R	vsym T-O		
H ₂ L ₂	-	-	-	-	-	1650	-
NaY	1009	677	440	610	745	-	-
Mn(L2)/NaY	1009	678	442	611	745	1630	-
Co(L2)/NaY	1009	678	440	609	745	1628	405-455, 550-580, 600-625
Ni(L2)/NaY	1009	677	440	610	745	1626	430-465, 600-620
Cu(L2)/NaY	1009	678	442	611	745	1625	360-395, 600-620

sulated in the zeolite nano cage did not show any significant shift in functional groups stretching bond of zeolite. Hence, in the free ligands, the band at ≈ 1650 arise from $\nu(\text{C}=\text{N})$ ²⁴ see Fig. 1. These latter stretching vibrations are shifted to lower frequencies about 1624-1630 cm^{-1} upon coordination²⁵⁻²⁷ through azomethine nitrogen.

The diffuse reflectance of complexes when incorporated on to zeolite are almost similar to alone complex indicating that maintain their geometry even after encapsulation without significant distortion. The electronic spectra of ligand showed a $n \rightarrow \pi^*$ transition at the 270-290 nm region assignable to the phenyl rings;²⁸ this energy is raised by ca. 10 nm in the complexes.²⁹ The spectrum of the Co(II) complexes exhibits two bands at 555-660 nm which are assigned to d-d transitions. In addition, lower energy absorption at 425 nm has been observed such low energy bands which have recently been shown to be characteristic of square-planar cobalt(II) chelates.³⁰⁻³⁴ The electronic spectrum of the Co (Schiff-base) incorporated onto zeolite exhibit three peaks at 405-445, 550-580 and 600-625 nm. We

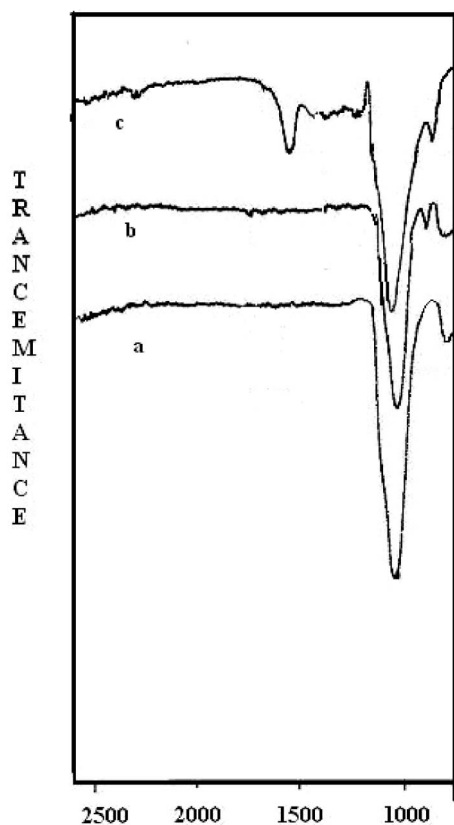


Fig. 1. FT-IR for (a) NaY, (b) [Co(II)]/NaY and (c) [Co(L)]/NaY.

have seen three peaks for Ni (Schiff-base) in nujol related ${}^1\text{A}_{1g} \rightarrow {}^1\text{A}_{2g}$ (ν_1), ${}^1\text{A}_{1g} \rightarrow {}^1\text{B}_{2g}$ (ν_2) and ${}^1\text{A}_{1g} \rightarrow {}^1\text{E}_g$ (ν_3) at 915, 605, 475 cm^{-1} respectively, corresponding to square-planar geometry. When Ni (Schiff-base) introduced to zeolite cage, DRS show two peaks at 430-465 and 600-620 nm. The electronic spectra of Cu(II) complexes show two bands near 650 nm (broad) and 400 nm (shoulder), attributed to ${}^2\text{B}_{1g} \rightarrow {}^2\text{A}_{1g}$, ${}^2\text{B}_{1g} \rightarrow {}^2\text{B}_{2g}$ and ${}^2\text{B}_{1g} \rightarrow {}^2\text{E}_g$ transitions for the former one and charge transfer for the latter one, indicating tetragonal configuration.³⁵ When these complexes incorporated onto zeolite, we have seen two peaks at 360-395 and 600-620 nm. The electronic spectrum of the Mn (Schiff-base) is indicated tetrahedral geometry similar visible spectra of known tetrahedral complexes containing oxygen-nitrogen donor atoms.³⁶ All of Metal (Schiff-base) show that the d-d transition band of complex are blue-shifted. It seems, the shifting of d-d band to the higher energy region clearly demonstrates that the in-plane ligand field around the metal ion is becoming stronger upon immobilization of the complex in NaY matrix than in its unimmobilized state³⁷ (Fig. 2).

Thermal analysis

Thermal behavior of pure zeolite, metal/zeolite and catalysts have been investigated by TGA and DTA (Fig. 3). The TGA curve of NaY zeolite shows 2 steps from 25-200 (4%) and 220-550 (12.5%) that these weight loss steps correspond to adsorption of physically and chemical water molecules and decomposition of zeolite or assigned to some sort of phase change, respectively which is a typical behavior for this compound. The endothermic peaks at 110 and 150 $^{\circ}\text{C}$ in DTA curve are assigned to desorption of physical and chemical water in NaY. The TGA and DTA curve of Mn(II)/Y shows two peak at 102 $^{\circ}\text{C}$ and 148 $^{\circ}\text{C}$ with about 5.8% weight loss, which are associated to dehydration of physically and chemically bonded water in sample, respectively. The TGA curves of Mn(L)/NaY shows four stage from 25 to 750 $^{\circ}\text{C}$, two stages with 8.495% weight loss related to desorption of water accompanied with endothermic peaks at DTA and third step with 8.733% weight loss is accompanied by exothermic effect in the DTA curve indicating the decomposition of the encapsulated complex onto zeolite. The TGA curve of activated Co(II)/Y zeolite shows about 6.1% weight loss upon heating to 200 $^{\circ}\text{C}$. This weight loss is accompanied by a broad endothermic peak in the DTA curve in the same tempera-

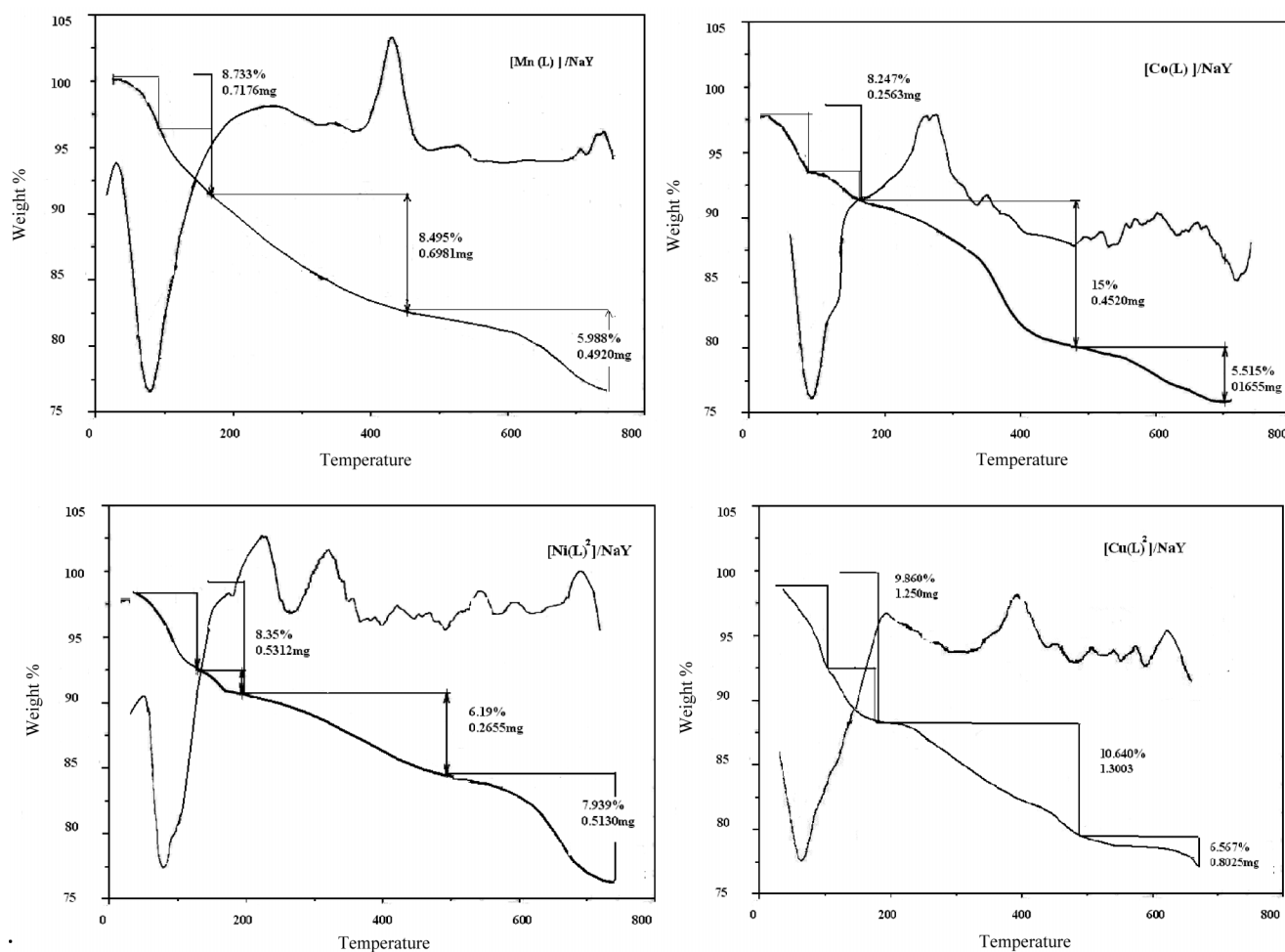


Fig. 2. TGA and DTA for Mn(L)/NaY, [Co(L)]/NaY, [Ni(L)]/NaY and [Cu(L)]/NaY.

ture range, suggesting that the weight loss is due primarily to the elimination of physically adsorbed and possibly chemically bonded water. In the case of Co(L)/NaY, the TG curve showed four stages of decomposition in the temperature range from 25 to 750 °C. The first two stages with 8.247% weight loss refer to the removal of the adsorbed water from the zeolite while the third stage from 190-485 °C with 15% weight loss is accompanied by exothermic effect in the DTA curve indicating the decomposition of the encapsulated complex and the last stage related to decomposition of zeolite. Thermal behavior of Ni(II)/Y and Cu(II)/Y similar to other samples, show only endothermic peaks with 3.5% and 4.1% weight loss, respectively, due the dehydration samples. Also TG curves for Ni(L)/NaY and Cu(L)/NaY have been shown four steps corresponds to a substantial loss of weight from 25 to 750 °C. Two stages until 200 °C with 8.35% and 9.860% weight loss for Ni(L)/

NaY and Cu(L)/NaY, respectively, accompanied with endothermic peaks are associated to dehydration of physically and chemically bonded water in samples. The third step of TGA in the temperature range from 190-490 °C (6.19% weight loss) and 200-400 °C (10.640%) for Ni(L)/NaY and Cu(L)/NaY, respectively, due the decomposition of the encapsulated complex that is accompanied by exothermic effect in the DTA curve. At least, the last steps with 7.939% and 6.567% weight loss until 750 °C for Ni(L)/NaY and Cu(L)/NaY, respectively, related to decomposition of zeolite.

Catalytic activity

The effect of transition metal complexes encapsulated in zeolite; [ML]-NaY was studied on the oxidation of benzyl alcohol to benzaldehyde and benzoic acid with TBHP in CH₃CN and the results are shown in Table 4. The

oxidation of benzyl alcohol is negligible in the absence of transition metal catalyst confirming that under the condition of the experiments, the oxidation is indeed catalytic in nature. The alone ligand were not catalytically activity. When we used from alone complex for oxidation, results show that we have decrease conversion about 5-10% without any change in selectivity. Also, the using of metal/NaY zeolite shows lower percent in conversation related to [ML]-NaY that confirms Schiff complexes really played the role. In agent test, the catalyst was filtered out after the experiment and lake of further reaction showed the absence of any catalytic active species in solution phase. The absence of complexes in solution was confirmed by testing for metal ions using atomic absorption spectrophotometer and we didn't have any changes in FT-IR spectra of [ML]-NaY zeolite. In order to investigate the catalytic activity of [ML]-NaY, the catalyst was separated from the reaction system by filtering and drying and followed by transfer to the next reaction recycle. As Table 5 shows, a rather stable conversion could be achieved after three reaction runs.

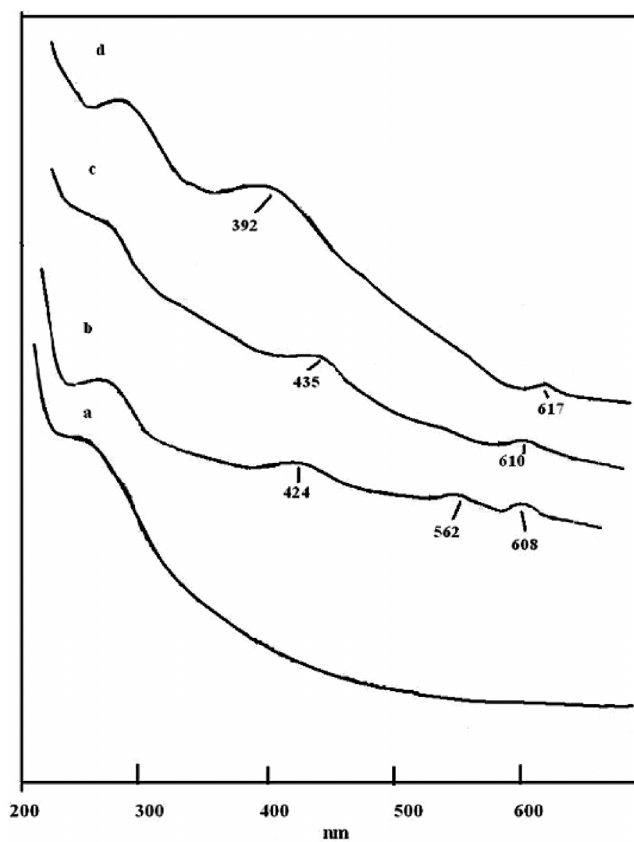


Fig. 3. DRS for (a) Mn(L)/NaY, (b) [Co(L)]/NaY, (c) [Ni(L)]/NaY and (d) [Cu(L)]/NaY.

Table 4. Oxidation of benzylalcohol with TBHP catalyzed by nanodimensional pores of zeolite-Y-encapsulated metal complexes in CH₃CN and reflux for 8 hours with 0.05 g catalyst

Catalyst	Conversion (%)	Selectivity (%)	
		Benzoic acid (%)	Benzaldehyde (%)
NaY	trace	trace	trace
H ₂ L ₂	-	-	-
[Mn(L)]/NaY	90.25	92.50	7.50
Mn/NaY	35.00	60.20	39.80
[Co(L)]/NaY	98.39	96.01	3.99
Co/NaY	41.50	70.96	29.04
[Ni(L)]/NaY	25.80	-	100.00
Ni/NaY	5.00	10.23	89.77
[Cu(L)]/NaY	92.64	95.00	5.00
Cu/NaY	38.30	69.01	30.99

Table 5. Catalytic activity after 3 run

Catalyst	Run	Conversion (%)
[Co(L)]/NaY	1	98.39
[Co(L)]/NaY	2	98.01
[Co(L)]/NaY	3	97.90
[Mn(L)]/NaY	1	90.25
[Mn(L)]/NaY	2	90.05
[Mn(L)]/NaY	3	88.95

Hence, results show that the increasing of catalyst (two times) does not have a significant effect on the percent of conversion under our study for reaction conditions. The catalyst [Co(L)]/NaY showed a higher activity with CH₃CN solvent compared to other solvents (Table 6). It seems that the formation of reactive catalyst complex-oxo intermediates in CH₃CN solution is prepared.³⁸ Literature review

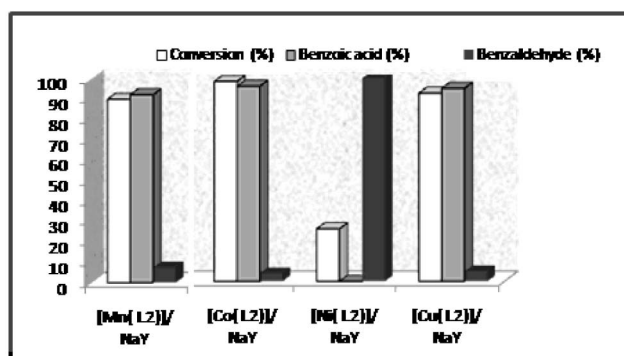


Fig. 4. Conversion and oxidation products of benzyl alcohol distributed in the acetonitrile with [M(L)]-NaY/TBHP.

shows that solvent plays an important role in catalytic behavior because it can make different phases uniform, thus promoting mass transportation, and could also change the reaction mechanism by affecting the intermediate species, the surface properties of catalysts and reaction pathways.^{14,39} The activity of benzyl alcohol oxidation decreases in the series [Co(L)]/NaY > [Cu(L)]/NaY > [Mn(L)]/NaY > [Ni(L)]/NaY. In several works, results for other catalyst such as metal oxide metal complex and M (Schiff base)/zeolite show that general production in oxidation of benzyl alcohol is benzaldehyde.^{17,40-42} In our work, the percent of product completely depends on catalyst when we used from Co(L)/NaY, Mn(L)/NaY and Cu(L)/NaY percent of benzoic acid is further and using Ni (Schiff-base)/NaY products of oxidation is Aldehyde. We assume that, the same as in Wang's work, the key point in the conversion of benzyl alcohol to benzoic acid is reduction of $L-M^{(n+1)+}$ to $L-M^{n+}$ (Scheme I). This reduction is simplified with ligands available around the metals.⁴³ It seems that the metals with stable $L-M^{(n+1)+}$ show a higher selectivity formation of benzoic acid. Hence, the preparation of benzoic acid by the further oxidation of benzaldehyde could be ef-

Table 6. The effect of different solvent in oxidation reaction, reflux for 8 hours with 0.05 g catalyst [Co(L)]/NaY

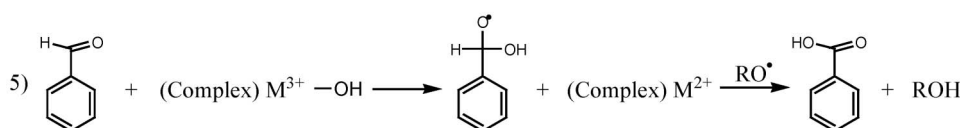
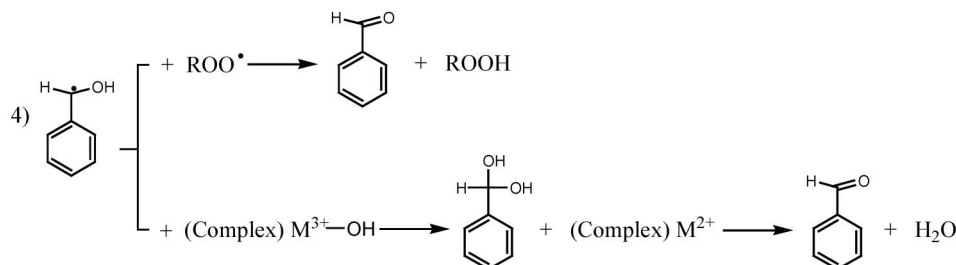
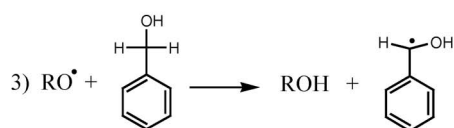
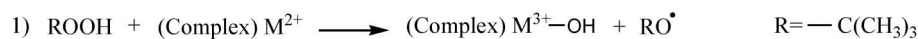
Different Solventes	Conversion (%)	Selectivity (%)	
		Benzoic acid (%)	Benzaldehyde (%)
Acetonitrile	98.39	96.01	3.99
Methanol	40.42	86.51	13.49
Chloroform	31.83	87.23	12.77
Dichloromethane	16.97	85.48	14.52

fectively avoided by using encapsulated system.

CONCLUSION

Y Zeolite-encapsulated, Mn(II), Co(II), Ni(II) and Cu(II) complexes of the N,N-bis(3,5-di-tert-butylsalicylidene)-2,2-dimethyl-1,3-diaminopropane ligands have been synthesized using the flexible ligand method. These encapsulated complexes exhibit fairly clear evidence in the XRD, surface area, pore volume, TGA and IR spectral characterization for the well-defined inclusion and distribution of complexes in the Y zeolite matrix. In the second section, we consider oxidation of cyclohexanol that cata-

Scheme I Mechanism conversion of benzyl alcohol to benzoic acid



lyzed by host-guest catalyst with tert-butyl hydrogen peroxide. Result shows that percent of product completely depend to catalyst because with using Co(L)/NaY, Mn(L)/NaY and Cu(L)/NaY percent of benzoic acid is further and using Ni (Schiff-base)/NaY products of oxidation are Aldehyde. At least, encapsulated complexes can be recovered and reused without the loss of catalytic activity.

Received January 27, 2010.

REFERENCES

- Smart, L.; Moore, E. *Solid State Chemistry*, 2nd ed., Chapman and Hall: London, 1995.
- Ozin, G. A.; Gil, C. *Chem. Rev.* **1989**, *89*, 1749.
- Herron, N. *Inorg. Chem.* **1986**, *25*, 4714.
- Jr., K. J.; Welch, A. A.; Gnade, B. E. *Zeolites* **1990**, *10*, 722.
- Kowalak, S.; Weiss, R. C.; Jr., K. J. *J. Chem. Soc. Chem. Commun.* **1991**, 57.
- Herron, N. *J. Coord. Chem.* **1988**, *19*, 25.
- Gabrielov, A. D.; Zakharov, A. N.; Romanovsky, B. V.; Tkachenko, O. P.; Shpiro, E. S.; Minachev, K. M. *Koord. Khim.* **1988**, *14*, 821.
- Zakharov, A. N.; Romanovsky, B. V.; Luca, D.; Sokolov, V. I. *Metalloorg. Khim.* **1988**, *1*, 119.
- Zakharov, A. N.; Romanovsk, B. V. *J. Incl. Phenom.* **1985**, *3*, 389.
- Balkus, Jr., K. J.; Gabrielov, A. G.; Bell, S. *Inorg. Chem.* **1994**, *33*, 67.
- Nishad Fathima, N.; Aravindhan, R.; Raghava Rao, J.; Unni Nair, B. *Chemosphere* **2008**, *6*, 1146.
- Rezaei, B.; Meghdadi, S.; Fazel Zarandi, R. *J. Hazard. Mater.* **2008**, *157*, 18.
- Salavati-Niasari, M. *J. Mol. Catal. A: Chem.* **2004**, *217*, 87.
- Salavati-Niasari, M. *Inorg. Chem. Commun.* **2004**, *7*, 963.
- Salavati-Niasari, M.; Bazarganipour, M. *Catal. Commun.* **2006**, *8*, 336.
- Salavati-Niasari, M.; Najafian, H. *J. Chem. Res.* **2003**, *9*, 536.
- Salavati-Niasari, M. *J. Mol. Catal. A: Chem.* **2006**, *245*, 192.
- Salavati-Niasari, M. *J. Mol. Catal. A: Chem.* **2008**, *283*, 120.
- Breck, D. W.; Tona Wanda, N. Y. Assigned to Union Carbide. Pat. No. 3,130,007, Patented April 21, 1964.
- (a) Larrow, J. F.; Jacobsen, E. N. *J. Org. Chem.* **1994**, *59*, 1939. (b) Khanmohammadi, H.; Salehifard, M.; Abnosi, M. H. *J. Iran. Chem. Soc.* **2009**, *6*, 300.
- Zendehdel, M.; Fouroughfar, N.; Gaykani, Z. *J. Inclusion Phenom. Macrocyclic Chem* **2005**, *53*, 42.
- Skrobot, F. C.; Rosa, I. L.; Paula, V. A.; Marques, A. P.; Martins, R.; Rocha, J.; Valente, A. A.; Iamamoto, Y. *J. Mol. Catal. A: Chem.* **2005**, *237*, 86.
- Barrer, R. M. *Hydrothermal Chemistry of Zeolite*; Academic Press: New York, 1982.
- Geary, W. J. *Coord. Chem. Rev.* **1981**, *7*, 81.
- Wang, R. M.; Feng, H. X.; He, Y. F.; Xia, C. G.; Sou, J. S.; Wang, Y. P. *J. Mol. Catal. A* **2000**, *151*, 253.
- Wang, R. M.; Hao, C. J.; Wang, Y. P.; Li, S. B. *J. Mol. Catal. A* **1999**, *147*, 173.
- Rao, S. N.; Munshi, K. N.; Rao, N. N. *J. Mol. Catal. A* **1999**, *145*, 203.
- Jaffe, H. H.; Orchin, M. *Theory and Application of Ultraviolet Spectroscopy*; Wiley: New York, 1962.
- West, D. X.; Salberg, M. M.; Bain, G. A.; Liberta, A. E. *Transition Met. Chem.* **1997**, *22*, 180.
- Lever, A. B. P. *Inorganic Electronic Spectroscopy*, 2nd ed., Elsevier: Amsterdam, 1984.
- Root, C. A.; Rising, B. A.; Vanderveer, M. C.; Hellmuth, C. F. *Inorg. Chem.* **1972**, *11*, 1489.
- Urbach, F. L.; Bereman, R. D.; Topido, J. A.; Hariharan, M.; Kalbacher, B. J. *J. Am. Chem. Soc.* **1970**, *92*, 792.
- Salavati-Niasari, M.; Ganjali, M. R.; Norouzi, P. *Trans. Met. Chem.* **2007**, *32*, 1.
- Salavati-Niasari, M. *Chem. Lett.* **2005**, *34*, 1444.
- Mostafa, S. I. *Transition Met. Chem.* **1998**, *23*, 397.
- Raman, N.; Raja, Y. P.; Kulandaisamy, A. *Proc. Indian Acad. Sci. (Chem. Sci.)* **2001**, *113*, 183.
- Dutta, B.; Jana, S.; Bera, R.; Kumar Saha, P.; Koner, S. *Appl. Catal., A* **2007**, *318*, 89.
- Mardani, H. R.; Golchoubian, H. *J. Mol. Catal. A: Chem.* **2006**, *259*, 197.
- Salavati-Niasari, M.; Sobhani, A. *J. Mol. Catal. A: Chem.* **2008**, *285*, 58.
- Xavier, K. O.; Chacko, J.; Mohammed Yusuff, K. K. *Appl. Catal., A* **2004**, *258*, 251.
- Tsuruya, Sh.; Miyamoto, H.; Sakae, T. I.; Masai, M. *J. Catal.* **1980**, *64*, 260.
- Furukawa, M.; Nishikawa, Y.; Nishiyama, S.; Tsuruya, Sh. *J. Mol. Catal. A: Chem.* **2004**, *211*, 219.
- Wang, M.; Hao, C. J.; Wang, Y. P.; Li, S. B. *J. Mol. Catal. A: Chem.* **1999**, *147*, 173.